JOURNAL OF PROTEOMICS 75 (2012) 5564–5577

Available online at www.sciencedirect.com

SciVerse ScienceDirect

www.elsevier.com/locate/jprot

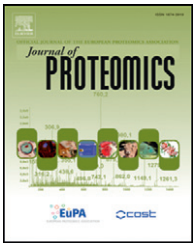

Quantitative proteomic analysis of differentially expressed proteins in the toxicity-lost mutant of *Alexandrium catenella* (Dinophyceae) in the exponential phase

Da-Zhi Wang, Cheng Li, Yong Zhang, Yu-Yu Wang, Zhi-Ping He, Lin Lin, Hua-Sheng Hong*

State Key Laboratory of Marine Environmental Science/College of the Environment and Ecology, Xiamen University, Xiamen 361005, China

ARTICLE INFO

Article history:
Received 5 May 2012
Accepted 1 August 2012

Keywords:
Dinoflagellates
Alexandrium catenella
Paralytic shellfish toxin
Biosynthesis
Quantitative proteomics
Two dimensional fluorescence differential gel electrophoresis

ABSTRACT

Alexandrium catenella is a widely spread dinoflagellate species which can produce potent neurotoxins and result in paralytic shellfish poisoning. To date, the molecular mechanisms regulating toxin biosynthesis remain unclear. This study compared protein profiles of a toxicity-lost mutant of *A. catenella*, ACHK-NT and its wild-type, ACHK-T in the exponential phase, using two dimensional differential gel electrophoresis and MALDI-TOF–TOF mass spectrometry. Morphological analysis showed that both subcultures were morphologically identical with the distinctive taxonomic characteristics of *A. catenella*. Sequence analyses of ITS1, 5.8S, ITS2 and 18S demonstrated that the mutant and wild subcultures were genetically identical for these markers. 90 differentially expressed protein spots were identified from ACHK-NT, of which 34 were down-regulated and 56 were up-regulated. Using a multilayered strategy for de novo protein sequence analysis, 67 proteins assigned to different functional categories were identified. Among them, 25 involved in bioluminescence, secondary metabolite biosynthesis, protein modification and toxin biosynthesis were down-regulated, while 42 participating in carbon fixation, stress response, transporter and protein folding were up-regulated. This study indicated that the strengthening of certain biological processes coupled with the depression of essential reactions upstream or downstream of the toxin biosynthetic pathway might have blocked toxin production and resulted in the loss of toxicity in the mutant *A. catenella*.

1. Introduction

Toxic dinoflagellates of the genus *Alexandrium* are the primary organisms responsible for harmful algal blooms (HABs) in the coastal waters of the world. Many *Alexandrium* species can produce potent neurotoxins that specifically and selectively bind the sodium channels on excitable cells, resulting in paralytic shellfish poisoning (PSP) in humans and other higher trophic level consumers [1]. It has been estimated that more than 2000 cases of human poisoning occur globally per year with a mortality rate of 15% [2]. PSPs have been considered as a serious toxicological health risk that may affect humans, other animals and ecosystems worldwide.

Much effort has been devoted to PSP toxin biosynthesis in *Alexandrium* as well as other PSP toxin-producing dinoflagellate species, and several biosynthesis pathways have been postulated. A few studies indicate that the toxin biosynthesis of dinoflagellates is regulated by genes, at least those interconverting enzymes which are encoded by nuclear genes [3]. The unusual distribution of the ability to produce PSP toxins might be explained by a rare event of horizontal gene transfer from bacteria to dinoflagellates [4]. It is postulated that the toxin

* *Corresponding author at:* State Key Laboratory of Marine Environmental Science, Xiamen University, Xiamen 361005, China. Fax: +86 592 2186055.
E-mail address: dzwang@xmu.edu.cn (D.-Z. Wang).

1874-3919/$ – see front matter © 2012 Elsevier B.V. All rights reserved.
http://dx.doi.org/10.1016/j.jprot.2012.08.001

biosynthesis pathway is identical in all PSP toxin-producing organisms, and that the corresponding genes should be homologous [5]. However, attempts to find genes associated with PSP toxin production in *Alexandrium* have remained inconclusive. The circadian time-frame of PSP toxin production has been elucidated in another dinoflagellate species, *Alexandrium fundyense* [6], however, the identification of candidate genes directly involved in PSP toxin production failed [7]. Subtractive hybridization analysis of cDNA reveals that the differential gene fragments between toxic and non-toxic subclones of *one Alexandrium tamarense* parental strain are directly related to toxins, as shown by polymorphism analysis of other subclones [3].

Recently, a PSP toxin gene cluster (sxt) has been revealed in a cyanobacterial species, *Cylindrospermopsis raciborskii* T3 [8]. This cluster encodes 26 proteins and a new type of polyketide synthase is demonstrated to initiate PSP toxin synthesis using arginine, S-adenosylmethionine (SAM) and acetate as primary precursors. Similar clusters are also found in other PSP toxin-producing cyanobacterial species [9,10]. A recent study on microarray-based comparisons of toxic and non-toxic strains *of Alexandrium minutum* reveals that 192 genes are more highly expressed in toxic *A. minutum* than in non-toxic *A. minutum*. However, no cyanobacterial PSP toxin genes are identified in toxic *A. minutum* although several unique genes are identified only in the toxic *A. minutum* [5]. Several SAM genes are successfully identified in dinoflagellates, but they are not directly correlated to PSP toxin biosynthesis [11]. Recently, the dinoflagellate transcripts of *sxtA*, the unique starting gene of saxitoxin (SXT) synthesis, are found to have the same domain structure as the cyanobacterial *sxtA* genes [12]. Although the identification of toxin-related genes or proteins has made a substantial contribution to understanding the molecular basis of toxin biosynthesis, the underlying mechanisms that regulate toxin biosynthesis are still unclear in dinoflagellates due to their unusual genome content and organization. Moreover, the PSP toxin genes in dinoflagellates might be different from their cyanobacterial counterparts as was shown in a recent study on gene transfer [4].

Proteins are the actual machinery that regulates cell growth, proliferation and homeostasis. It is logical, therefore, that the study of proteins should help uncover the toxin biosynthesis mechanisms in dinoflagellates. Global techniques such as proteomics provide effective strategies and tools for profiling and identifying the proteins of dinoflagellates [13,14]. Two dimensional difference gel electrophoresis (2D-DIGE) is a quantitative 2-D gel-based proteomic approach that employs three fluorescent succinimidyl esters, termed CyDyes, to differentially label proteins prior to electrophoretic separation [15]. The advantage of 2D-DIGE relies on defining statistical significance on proteins identified differentially expressed between control and treated samples. This technique has recently been applied to identify cell wall and cell surface proteins *of Alexandrium catenella* [16,17].

In our recent study, we found that a subculture of toxic *A. catenella*, named ACHK-NT, had lost the ability to produce toxin, indicating that mutation might have occurred in ACHK-NT. If this is the case, then the pair of toxic and non-toxic cultures provides an ideal experimental system to study the mechanisms potentially involved in toxin production. The present study applied 2D-DIGE to compare the protein profiles of *A. catenella* between the toxicity-lost mutant, ACHK-NT and its wild type, ACHK-T in the exponential phase, in order to reveal any differentially expressed proteins and their molecular functions. 67 proteins were successfully identified from 90 differentially expressed protein spots and these proteins were involved in various biological processes. The difference in these biological processes (i.e. from carbon fixation, to toxin and secondary metabolite biosynthesis) between the mutant and wild *A. catenella* might determine their toxin-producing capability. The strengthening of certain biological processes coupled with the depression of those toxin biosynthesis-related proteins might have blocked toxin production and resulted in the loss of toxicity in the toxin-lost mutant *A. catenella*.

2. Materials and methods

2.1. Organisms and culture conditions

Unialgal cultures of toxic and non-toxic *A. catenella* strains were provided by the Collection Center of Marine Bacteria and Algae, Xiamen University. The isolates are routinely maintained in K medium [18] at 20 °C under a 14:10 h light: dark photoperiod at a light intensity of approximately 100 μmol photons m^{-2} s^{-1} provided by fluorescent lamps.

A. catenella cells for 2D-DIGE comparison were grown in 5 L flasks containing 4 L of K medium, and the culture conditions were the same as above. When the cells entered the exponential phase, approximately 2×10^6 vegetative cells were harvested by centrifugation at 5000×*g* for 10 min at 20 °C. The pellet was subsequently transferred to a 1.5 mL microcentrifuge tube, rinsed twice with sterile seawater, and centrifuged again at 5000×*g* for 30 min at 20 °C. The pellets were stored at −80 °C until protein extraction.

2.2. Morphology analysis

For scanning electron microscope (LEO 1530 Gemini, Zeiss/LEO, Oberkochen, Germany) analysis, cells were harvested at the exponential phase and fixed with osmic acid at a final concentration of 1%. The fixed cells were dehydrated in gradient concentrations of ethanol, critical-point dried, and sputtered with gold. Observation and photography were carried out at an accelerating voltage of 20 kV. For fluorescence microscopic analysis, approximately 50 vegetative cells for each strain were stained with Calcofluor white following the method of Fritz and Triemer [19], and examined and photographed under an Olympus microscope (BX51, Olympus, Tokyo, Japan) with a CCD camera.

2.3. DNA extraction, amplification and sequencing

50 mL of each subculture was harvested by centrifugation at the exponential growth phase. DNA was extracted using the CTAB method following the protocol of Wang et al. [14]. The total ITS1–5.8S–ITS2 region was amplified in a PCR thermocycler using ITSA and ITSB primers [20]. The procedure for the PCR reaction was 4 min at 94 °C, followed by 25 cycles of 1 min

at 94 °C, 2 min at 50 °C, 3 min at 72 °C, and a final extension of 7 min at 72 °C [14]. The PCR product was sequenced directly on an ABI 377 automated DNA sequencer. The sequence data were evaluated using the BLAST program [21] against published sequences in GenBank.

2.4. PSP toxin analysis

For ACHK-NT, at least 3×10^8 algal cells from triplicate samples were collected in the exponential phase. For ACHK-T, approximately 5×10^4 algal cells from triplicate samples were collected using centrifugation at 2500×*g* for 5 min every day, followed by subsequent re-suspension in 0.5 mL of 50 mM acetic acid, then followed by homogenization with three successive sonication cycles. 20 mL of the supernatant obtained after centrifugation at 20,000×*g* for 30 min was subjected to toxin analysis, which was carried out using high-performance liquid chromatography (HPLC) with fluorescence detection using reverse phase chromatography with post column derivatization and an Intersil C8-5 column (15 cm×4.6 cm), as described previously [22]. Toxin standards for gonyautoxin (GTX), STX, neo-STX and C1/C2, bought from the National Research Council, Canada, were used for identification and quantification of PSP toxins. Three mobile phases (with a flow rate of 0.8 mL min^{-1}) were used for the separation of different toxin groups: (1) 2 mM tetrabutyl ammonium phosphate solution adjusted to pH 6.0 with acetic acid for C toxins; (2) 2 mM 1-heptanesulfonic acid in 10 mM ammonium phosphate buffer (pH 7.1) for the GTX group; and (3) 2 mM 1-heptanesulfonic acid in 30 mM ammonium phosphate buffer (pH 7.1): acetonitrile (100:5) for the STX group.

2.5. Protein extraction

Protein extraction was performed using the Trizol method according to the manufacturer's instructions and protocol. Briefly, 1 mL Trizol reagent was added to the cell pellet and it was subjected to sonication on ice. Subsequently, 200 μL of chloroform was added to the cell lysate before shaking vigorously for 15 s. The mixture was allowed to stand for 5 min at room temperature before being centrifuged at 12,000×*g* for 15 min at 4 °C. The top pale-yellow or colorless layer was removed, and then 300 μL of ethanol was added to resuspend the reddish bottom layer, and the mixture was centrifuged at 2000×*g* for 5 min at 4 °C. The supernatant was transferred to a new tube, 2 mL of isopropanol added and the mixture was allowed to stand for at least 1 h for precipitation of proteins at −20 °C. It was then centrifuged at 14,000×*g* for 30 min at 4 °C. The pellet obtained was briefly washed with 95% ethanol before being allowed to air dry, after which 30–100 μL of lysis buffer (pH 8.5, from DIGE protocol) was added to solubilize the protein pellet. Protein quantification in the urea-containing protein samples was performed using the 2D Quant kit (GE Healthcare, USA).

2.6. 2D-DIGE analysis

The pH of each protein sample was adjusted to pH 8.5 with lysis buffer (pH 9.5, from the DIGE protocol) if required. For the DIGE experiment, 50 μg of protein from each *A. catenella* strain was incubated with 400 pmol (in 1 μL of anhydrous DMF) of cyanine Cy3 or Cy5 (GE Healthcare, USA). Samples were run in triplicate with a label switch so as to avoid labeling bias. The pooled internal standard, for gel normalization, was prepared containing an equal protein quantity of each of the six samples and labeled with Cy2. The reaction was performed for 30 min on ice in the dark and was stopped by adding 10 mM lysine for 10 min on ice. Prior to electrophoretic separation, 50 μg of the Cy2-labeled pooled internal standard was added to equal amounts of a Cy3- and Cy5-labeled sample. Onto each gel 150 μg of protein was loaded and separated using 2-D gel electrophoresis. Samples from each strain were run in duplicate. First dimension gel electrophoresis was carried out using a 24 cm Immobiline Dry Strip with a linear pH 4–7 gradient (BioRad) and an Ettan IPGphor 3 IEF System (GE Healthcare) set at 20 °C. Strips were rehydrated in a solution containing 7 M urea, 2 M thiourea, 4% CHAPS, 1% DTT and 0.5% v/v IPG buffer 4–7. Isoelectric focusing was performed in seven steps: at 40 V for 6 h, at 100 V for 6 h, at 500 V for 30 min, at 1000 V for 1 h, at 2000 V for 1 h, at 10,000 V for 1.5 h and at 10,000 V for 60,000 V·h. After equilibrating in a solution containing 6 M urea, 2% SDS, 50 mM Tris–HCl (pH 8.8), 30% glycerol, and 1% DTT, or 2.5% iodoacetamide (17 min of incubation in both cases), strips were ready to be applied to the second dimension gels (12.0% SDS-PAGE). The separation was performed in an Ettan Dalt system (GE Healthcare) at 1 w/gel for 30 min and then at 15 w/gel until the dye reached the very bottom of the gel.

2.7. Image capture and analysis

Cy2-, Cy3- and Cy5-labeled protein images were produced by excitation of gels at 488, 532 and 633 nm, and emission at 520, 590 and 680 nm, respectively, using a DIGE Imager (GE Healthcare). Gel images were cropped using the ImageQuant TL software program and analyzed using the DeCyder™ 2-D Differential Analysis software v6.5 (GE Healthcare). Firstly, the Cy2, Cy5, and Cy3 images were merged for each gel, allowing the co-detection of spot boundaries on the three images. For each spot, the spot volume (sum of pixel intensities) was calculated in the Cy3 or Cy5 channels then normalized according to the corresponding Cy2 spot volume. The gel chosen for picking was fixed (40% ethanol, 10% acetic acid) for at least 2 h, and stained using the silver staining method [23].

2.8. In-gel digestion of proteins

In-gel digestion of proteins was performed using a modified protocol for the preparation of silver-stained 2D protein spots for in-gel tryptic digestion [24]. The entire slab of a two-dimensional gel was rinsed with water for a few hours, put into a plastic tray with the gel, placed onto a light box and spots of interest were excised with clean pipette tips. The gel pieces were transferred into an Eppendorf microcentrifuge tube, then washed with water before destaining for 10 min. Destaining the gel pieces involved shaking the tubes for 5 min with 200 μL of destaining solution (15 mM $FeK_3(CN)_6$, 50 mM $Na_2S_2O_3$). The destaining solution was removed and the gel pieces were washed three times with 800 μL water, and vortexed for 10 min for a total of 30 min at 50 °C. Next, 200 μL

of neat acetonitrile was added and the gel pieces were incubated at room temperature with occasional vortexing, until they became white and shrunk. They were then removed from the acetonitrile. Sufficient trypsin buffer (typically, 5 ng/μL Promega sequencing grade modified trypsin in 10 mM NH_4HCO_3, trypsin concentration depending on the loading quantities of protein in 2D gel) was added to cover the dry gel pieces and they were placed in an ice bucket or a fridge. After 30 min saturation, the gel pieces were checked for complete rehydration and the redundant trypsin outside the gel pieces was removed. Then, 5–10 μL of 10 mM ammonium bicarbonate buffer was added to cover the gel pieces and keep them immersed during enzymatic cleavage. The tubes with their gel pieces were placed in an air circulation thermostat and incubated at 37 °C for 4 to 16 h.

2.9. MALDI-TOF–TOF analysis

Protein identification was performed on an AB SCIEX MALDI TOF–TOF™ 5800 analyzer (AB SCIEX, Foster City, CA) equipped with a neodymium:yttrium–aluminum-garnet laser (laser wavelength 349 nm). TOF/TOF calibration mixtures (AB SCIEX) were used to calibrate the spectrum to a mass tolerance within 150 ppm. For the MS mode, peptide mass maps were acquired in positive reflection mode, and the 850–4000 m/z mass range was used with 1000 laser shots per spectrum. The PMF peak detection criteria used were a minimum S/N of 10, a local noise window width mass/charge (m/z) of 250 and a minimum full-width at half-maximum (bins) of 2.9. A maximum of 20 precursors per spot with a minimum signal/noise ratio of 50 were selected for MS/MS analysis using ambient air as the collision gas with medium pressure of 10^{-6} Torr. The contaminant m/z peaks originating from human keratin, trypsin autodigestion, or the matrix were excluded from the MS/MS analysis. An energy of 1 kV was used for collision-induced dissociation, and 2000 acquisitions were accumulated for each MS/MS spectrum. The peak detection criteria used were a minimum S/N of 3, a local noise window width (m/z) of 200 and a minimum full-width at half-maximum (bins) of 2.9. A combined MS and MS/MS search was performed against the NCBInr database with no taxonomic restriction (updated December, 2010, containing 4,607,655 entries). All database searches were fulfilled using the GPS Explorer™ software (version 3.6, AB SCIEX) running a Mascot search algorithm (v2.2, Matrix Science, London, UK) for protein identification. Protein identification was conducted using multi-layered workflow integrated mass spectra processing with conventional and homology-based searches [14]. Briefly, Mascot, a highly specific stringent search, was applied as the first layer screen to identify either known proteins or unknown proteins sharing identical peptides presented in a database. Once the confident identifications were removed after searching against the NCBInr database, the rest were searched against the dinoflagellate expressed sequence tag database. In the last layer, borderline and non-confident hits were further subjected to de novo interpretation using the DeNovo Explorer™ software. The de novo sequences passing a reliability filter were subsequently submitted to non-redundant MS-BLAST searches. Only high-scoring segment pairs (HSSPs) with a score of 62 or above were considered to be confident.

2.10. Bioinformatic analysis

The identified proteins were converted to their corresponding homologous GI numbers and imported into the searching web of a protein information resource (http://pir.georgetown.edu/pirwww/search/batch.shtml), and multiple entries were retrieved from the iProClass database. The protein sequence of those retrieved with GI numbers was then submitted to the Automatic Annotation Server ver. 1.64a of KEGG in FASTA format, and the GO functional categories were analyzed according to the results of the retrieval in the iProClass database, and to Toulza et al. [25].

3. Results

3.1. Morphology and ITS sequence analyses of the mutant and wild A. catenella

The thecal plates of mutant and wild subcultured cells stained with Calcofluor revealed that the two subcultures presented the typical plate tabulation of *A. catenella* (Po, SA, 1'). The apical pore complex was broad, triangular and widened dorsally (Fig. 1D), no ventral pore was observed in the first apical plate and the Po had a strongly developed callus (Fig. 1).

Complete ITS1, 5.8S, ITS2 and 18S were amplified and a single band of ca. 600 bp was obtained from the two subcultures (Fig. 2). Direct sequencing of PCR products showed that the two subcultures of *A. catenella* shared an identical ITS and 18S sequence, but displayed ambiguity in one position (177th) of ITS1.

3.2. Growth and toxin profiles of the mutant and wild A. catenella

Difference in cell growth was observed between mutant and wild *A. catenella* grown in K medium (Fig. 3). ACHK-NT exhibited consistently high growing capability and high cell density. The maximum cell density reached approximately 11,400 cells/mL for ACHK-NT versus 9500 cells/mL for ACHK-T.

The typical HPLC profiles of toxin extracts from the mutant and wild *A. catenella* are shown in Fig. 4. They presented remarkable differences. The chromatograms obtained from ACHK-T showed a toxin profile consisting of C1, C2 (N-sulfocarbomoyl toxin), GTX1 and dcSTX, but no other PSP toxin derivatives were detected. The toxin content (fmol/cell) of ACHK-T ranged between 2.52 and 18.49 fmol/cell with the highest value in the late exponential phase (Supplemental Fig. 1). In contrast, no C1, C2, GTX1, dcSTX or any other PSP toxin derivative was detected in the ACHK-NT extract even when prepared with quite high cell density (3×10^8 cells), indicating that ACHK-NT had lost the ability to produce PSP toxins.

3.3. 2D-DIGE analysis of protein profiles

Proteins prepared from mutant and wild (as the reference) *A. catenella* cells in the exponential growth phase were labeled with different fluorescent dyes, separated by 2D-PAGE, and the expression of the resolved protein spots was quantitatively

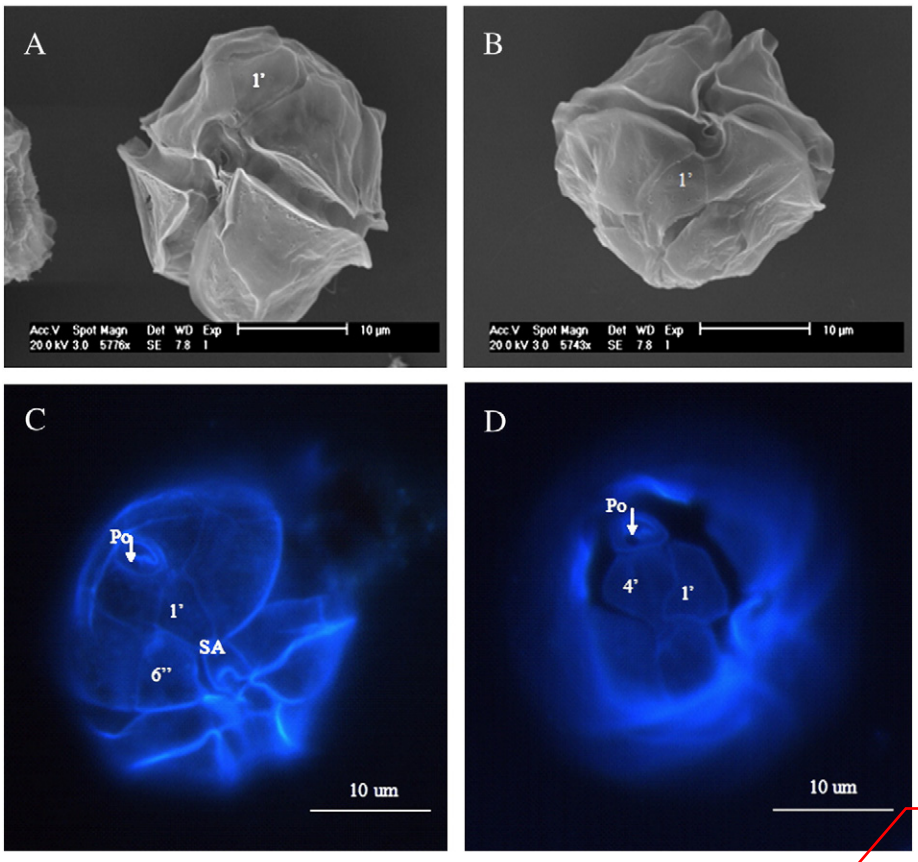

Fig. 1 – Fine structure of *A. catenella* under SEM and LM. (A) and (B) whole cell of *A. catenella* (SEM); (C) apical showing the first apical plate (1'), location of the apical pore plate (Po arrowhead) and anterior sulcal plate (SA); (D) apical view of *A. catenella* (LM), and the first apical plate (1') without a ventral pore.

analyzed by scanning the fluorescent intensity of the labeled protein spots. The representative 2D-DIGE images of both are shown in Fig. 5. Generally, the protein expression patterns of mutant (Fig. 5A) and wild (Fig. 5B) *A. catenella* cells were identical and no unique protein spots were found exclusive to ACHK-T or ACHK-NT. However, 90 protein spots presented more than 1.5 fold changes in abundance (p-value <0.05) between mutant and wild *A. catenella* subcultures (Supplemental Fig. 2). Among these protein spots, 34 were down-regulated while 56 were up-regulated in ACHK-NT.

Fig. 2 – Nucleotide polymorphism for the ITS sequence in the two subcultures of *A. catenella*. The base pair difference between toxic and non-toxic subcultures is highlighted.

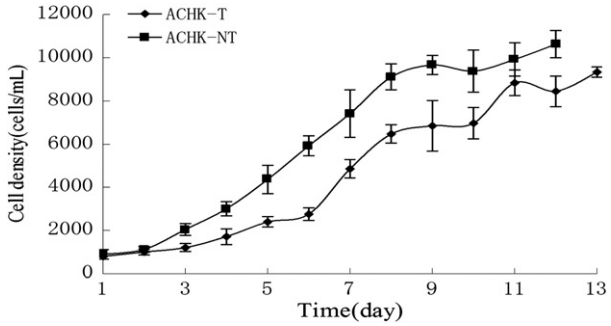

Fig. 3 – Growth curves of ACHK-T and ACHK-NT under optimal growth conditions.

3.4. *Characterization of differentially expressed proteins*

The differentially expressed protein spots were manually excised from gels and identified using MALDI-TOF/TOF MS. 35 protein spots were confidently identified against the NCBInr database using the multi-layered identification method, while 13 protein spots were identified against dinoflagellate EST. The remaining 42 protein spots with non-confident hits were further subjected to de novo interpretation using the DeNovo Explorer™ software combing non-redundant MS-BLAST searches, and 19 proteins were tentatively identified with HSSPs (Supplemental file). However, 23 protein spots did not obtain positive identification and were assigned to unknown proteins. It was noted that a few protein spots were identified as the same protein with different MW and/or *p*I values. These proteins might represent different modifications of the same gene product or isoforms of the same protein family.

The identified proteins were functionally categorized using Automatic Annotation Server ver. 1.64a of KEGG (Fig. 5). The down-regulated proteins in the ACHK-NT were classified into nine categories, mainly involved in bioluminescence, secondary metabolite biosynthesis, protein modification and toxin biosynthesis. The up-regulated proteins in the ACHK-NT were assigned into 13 groups, implicated primarily in carbon fixation, stress response, transporter and protein folding. The NCBI accession number, protein name, protein score, C.I. %, total ion score and C.I. %, number of unique peptides and total spectra used in the identification, and the theoretical MW and isoelectric point of the proteins identified are listed in the Supplemental file.

3.5. *Differentially expressed proteins in ACHK-NT*

The proteins with enhanced expression in ACHK-NT fell into 13 major biological process groups (Fig. 6 and Table 1). Among them, seven proteins were involved in carbon fixation, comprising chloroplast transketolase, chloroplast phosphoribulokinase, fructose-bisphosphate aldolase and phosphoenolpyruvate carboxykinase. Seven proteins were assigned with stress responses, including heat shock protein (HSP) 70, HSP90, ferritin and Dps. Five proteins were designated as transporter proteins, including transitional endoplasmic reticulum ATPase protein, magnesium chelatase ATPase subunit I, ATP synthase and ABC transporter related protein. Three proteins involved in the carbohydrate metabolic process, i.e. glyceraldehyde-3-phosphate dehydrogenase type I, hypothetical protein CHLNCDRAFT_56532 and phosphoenolpyruvate synthase were identified. Additionally, several other proteins participate in carbon utilization, the oxidation-reduction process, oxidative phosphorylation, the macromolecule catabolic process, photophosphorylation, protein synthesis, regulation of biological processes, the TCA cycle, and amino acid metabolism. In addition, seven unclassified proteins were enhanced in ACHK-NT.

The down-regulated proteins in ACHK-NT were classified into nine major biological process groups (Fig. 6 and Table 1). Among them, nine isoforms of luciferin-binding protein (LBP), a key protein involved in bioluminescence, were found to be significantly suppressed in ACHK-NT. Another significantly suppressed protein was polyketide synthase which belongs to secondary metabolite biosynthesis. GAF sensor hybrid histidine kinase and hybrid signal transduction histidine kinase J belonging to the same family of histidine kinase were also down-regulated in ACHK-NT. In addition to these proteins, a number of other proteins related to the chaperone, cofactor metabolic, heterocycle metabolic, oxidation-reduction, protein modification and translation processes were also found to be depressed in ACHK-NT.

4. Discussion

Over the past few decades, the origin, chemical structure, and toxicity of PSP toxins from dinoflagellates have been well elucidated. However, the enzymes or proteins directly involved in the biosynthesis and metabolism of the PSP toxins remain unknown. Understanding the mechanisms of toxin production and breakdown is therefore fundamental to further PSP research and to this end, in this study, we compared the protein profiles of a toxicity-lost mutant and a wild *A. catenella* and identified differentially expressed proteins using a quantitative proteomic approach.

4.1. *The origin and features of the mutant A. catenella*

ACHK-T is a single clone isolated from the South China Sea and has been routinely maintained in different laboratories for many years. Recently toxicity examination demonstrated that one subculture (ACHK-NT) had lost the ability to produce PSP toxins. Based on comparison with PSP toxin standards, no PSP derivative chromatograms were found in this ACHK-NT even at high cell density (3×10^8 cells), which was 6×10^3-fold that of toxic cells (5×10^4 cells). To exclude the possibility of contamination by other cultures, morphological and sequence analyses of different rRNA domains were conducted

Fig. 4 – High performance liquid chromatography of the paralytic shellfish toxin profiles of ACHK-T and ACHK-NT. (A) C1, C2 toxins; (B) GTX1 toxin; and (C) dcSTX toxin. The Y-coordinate is retention time (min), and the X-coordinate is fluorescence intensity (LU).

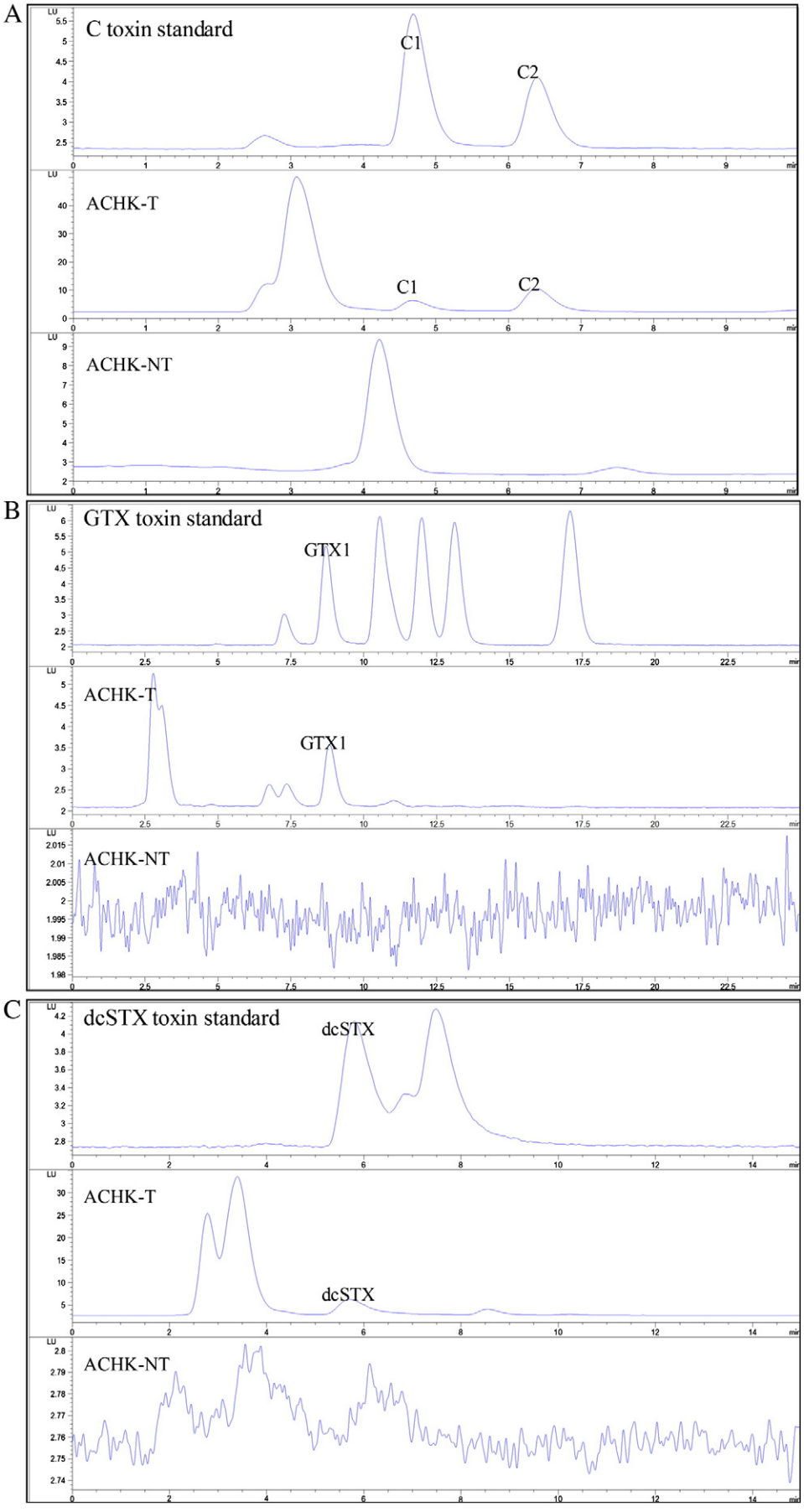
A
C toxin standard
C1
C2
ACHK-T
C1
C2
ACHK-NT
B
GTX toxin standard
GTX1
ACHK-T
GTX1
ACHK-NT
C
dcSTX toxin standard
dcSTX
ACHK-T
dcSTX
ACHK-NT

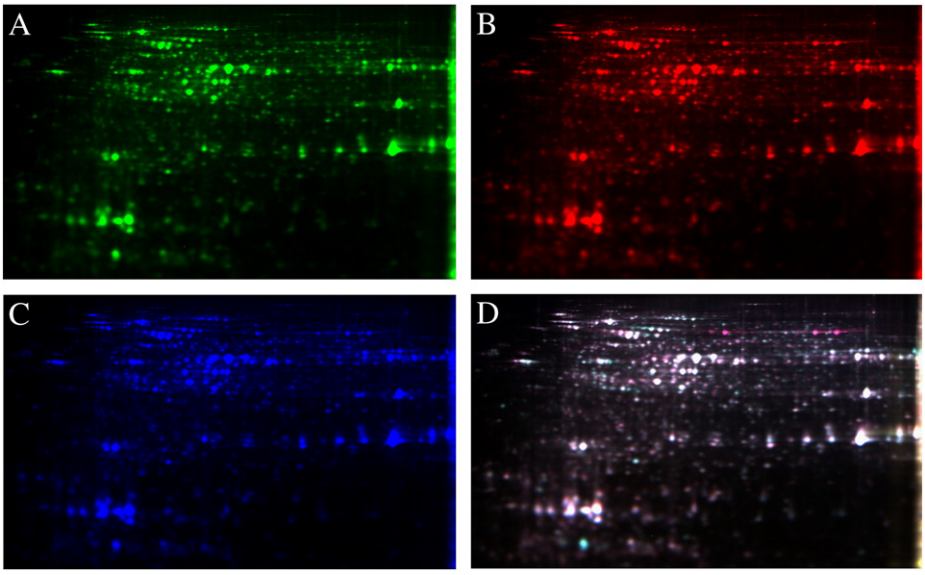

Fig. 5 – Representative image of 2-D DIGE of *A. catenella*. ACHK-T and ACHK-NT proteins were labeled with DIGE Fluor dyes, and separated on a linear IPG strip (pH 4–7, 24 cm) in the first dimension and on a 12% SDS-polyacrylamide gel in the second dimension. The gel was scanned with an Ettan™ DIGE Imager. Pseudocolors were used for each DIGE Fluor dye. (A)–(C) images for ACHK-NT labeled with Cy3 (green), ACHK-T with Cy5 (red), and internal standard with Cy2 (blue), respectively. (D) superimposed images from Cy2, Cy3, and Cy5 labeled proteins. (For interpretation of the references to color in this figure legend, the reader is referred to the web version of this article.)

in this study and demonstrated that both the toxic and non-toxic subcultures were identical to *A. catenella* but they presented different cell growth capacities with the mutant ACHK-NT growing faster than the wild ACHK-T as well as having a higher cell yield. This result demonstrated that the mutation which had occurred in ACHK-NT cells had resulted in the alteration in both growth capacity and toxin producing ability. The exact reasons for this mutation of *A. catenella* are not clear. The loss of toxicity in a dinoflagellate species, *Alexandrium lusitanicum*, might be caused by long term exposure to antibiotics during culture maintenance, which also affects the cell growth capacity [26]. Artificial maintenance conditions can also result in variations of toxin composition and toxicity [27]. Under these conditions, mutations and irreversible physiological changes are likely to occur, resulting in permanent changes in the algal activities at both biochemical and genetic levels, including elevated rates of toxin biosynthesis. Other studies show that toxic and non-toxic subclones of *A. tamarense* co-exist in seawater and variations of environmental or culture conditions might be one of the key factors resulting in the survival of toxic or non-toxic subcultures [3,28]. A significant variation in toxicity (more than a 10^4-fold difference) is reported in the cellular toxin content of toxic and non-toxic samples of *A. tamarense* [3]. A similar study also reports up to a 100-fold variation in toxicity among isolates of motile cells and 20-fold for subcultures from a single clonal culture [29]. These studies suggest that the ability to produce toxins varied significantly among different strains, subcultures or subclones, and that toxicity loss could occur under certain culture conditions.

4.2. *Enhanced photosynthetic carbon fixation in the mutant A. catenella*

The majority of proteins identified as being up-regulated in ACHK-NT are related to cellular metabolism. The significantly

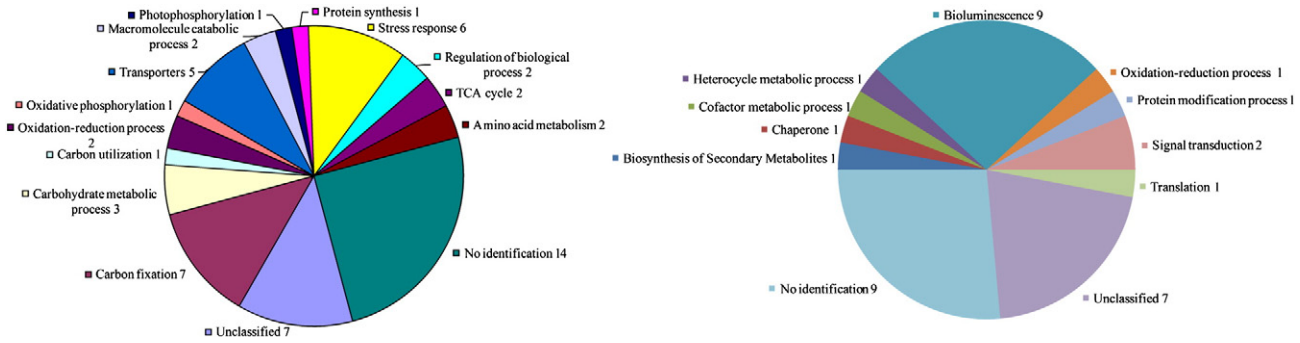

Fig. 6 – The GO functional categories of the up-regulated (left pie) and down-regulated (right pie) proteins in ACHK-NT compared to ACHK-T. The functional categories were defined according to Toulza et al. [25].

up-regulated protein was a light-harvesting protein (LHP) which is a photophosphorylation protein involved in photosynthesis. LHP helps to harvest more of the incoming light than would be captured by the photosynthetic reaction center alone in photosynthetic organisms [30]. Three main reactions occur in the light-dependent stage: electron transport, redox reactions and photophosphorylation. These reactions are reliant on the ability of photons to raise the energy of electrons which allows for transfer of the electron down an electron chain allowing redox reactions to occur. Up-regulation of LHP might result in more photons being able to participate in the reactions, and in turn these redox reactions allow for the synthesis of more ATP and NADPH that are rich in energy and crucial in the carbon fixation from carbon dioxide which occurs in the light-independent stage. So it is not surprising that several proteins participating in the carbon fixation, i.e. fructose-bisphosphate aldolase, chloroplast transketolase, chloroplast phosphoribulokinase and phosphoenolpyruvate carboxykinase, were enhanced in the mutant ACHK-NT. Among them, transketolase is one of the enzymes having significant control over carbon fixation, and the enhancement of this enzyme may lead to an increase of photosynthetic carbon assimilation, while the suppression of transketolase activity inhibits the biosynthesis of aromatic amino acid and intermediates of the shikimic acid pathway, and, subsequently, leads to a decline in the total biomass yield of plants [29]. In the present study, the up-regulation of transketolase as well as other carbon fixation related proteins might have contributed to the high growth capability and cell density of ACHK-NT.

In photosynthesis organisms, carbon fixation is the first step of a series of biochemical reactions in the Calvin cycle. In this study, two proteins, glyceraldehyde-3-phosphate dehydrogenase (type I) and chloroplast phosphoribulokinase, both involved in the Calvin cycle and photophosphorylation, were up-regulated in the mutant ACHK-NT, indicating that carbon fixation was enhanced in the mutant *A. catenella*. The enhancing expression of these proteins might also explain the fast growth and high cell density (growth capability) observed in ACHK-NT.

Carbon fixation and nitrogen assimilation are two coupled processes in photosynthetic organisms. Nitrate assimilation can only proceed to completion when carbon assimilation provides the carbon skeletons for amino-acid formation, and lack of these may lead to accumulation of toxic nitrites in the algal cells. Thus, up-regulation of carbon fixation related proteins might enhance the assimilation of nitrate and compel more N-containing compounds to synthesize amino acids for cell growth, which in turn limits PSP toxin biosynthesis (Fig. 8), since PSP toxins are a group of N-rich compounds (ca. 30% by weight) which are synthesized during N-upshock [31,32]. It is estimated that as much as 5 to 15% of the total cellular N is bound to PSP toxins in some highly toxic species [33]. The toxin content is dependent on the cellular N status of nitrate grown cells, suggesting that the competition for N in toxin production with other metabolic pathways such as growth may affect the toxin biosynthesis ability. The enhancement of carbon fixation in ACHK-NT might invest more intracellular N-compounds in cell growth and related physiological processes rather than in toxin production (Fig. 7).

4.3. *Suppressed biological processes related to toxin biosynthesis in the mutant A. catenella*

Recently the gene cluster involved in PSP toxin biosynthesis has been characterized from cyanobacteria [8,9]. Twenty-six genes are involved in toxin biosynthesis and 13 of them are unique in toxin-producing cyanobacteria. However, genetic information concerning PSP toxin biosynthesis in dinoflagellates still remains elusive. Several studies demonstrate that removal of bacteria from *Alexandrium* cultures does not eliminate toxin production [34–36], which supports the conclusion that the dinoflagellate gene is responsible for PSP toxin production. Stüken et al. show that the genes required for SXT synthesis are located in the nucleus of dinoflagellates and the dinoflagellate transcripts of *sxtA* have the same domain structure as the cyanobacterial *sxtA* gene, the unique starting gene of SXT synthesis [12]. In our study, polyketide synthase encoded by *sxtA* was identified to be down-regulated in ACHK-NT. Polyketide synthase is demonstrated to initiate the PSP toxin synthesis using arginine, SAM and acetate as primary precursors in cyanobacteria. The down-regulation of polyketide synthase might decrease the ability of ACHK-NT to biosynthesize toxins. Moreover, two other toxin-related proteins (histidine kinase and chaperone-like protein encoded by *sxtZ* and *sxtE* genes, respectively, in cyanobacteria [4,8]) were also identified in our study. GAF sensor hybrid histidine kinase and hybrid signal transduction histidine kinase J are two histidine kinase isoforms, which were suppressed in ACHK-NT, while D2, the homologue of chaperone-like protein, was also down-regulated in ACHK-NT. The suppression of these proteins might result in those precursors for PSP toxin biosynthesis entering other metabolic pathways which blunts the biosynthesis of PSP toxin in ACHK-NT (Fig. 8).

In addition to those proteins directly participating in toxin biosynthesis, some proteins up-regulated in ACHK-NT might indirectly depress or block essential reactions upstream or downstream of the biosynthetic pathway of PSP toxins (Fig. 8). Dihydrolipoamide succinyltransferase, which was identified to be up-regulated in ACHK-NT, catalyzes the α-ketoglutarate, CoA-SH and NAD+ reaction by oxidative decarboxylation. In cyanobacteria, *sxtS* catalyzes the conversion of compound D' [7], α-ketoglutarate and O_2 to succinate, CO_2 and an intermediate in the sixth step of the PSP toxin biosynthesis pathway. Thus, α-ketoglutarate plays an important role in the above two biological processes as an essential substrate. In our study, the up-regulation of dihydrolipoamide succinyltransferase might compete for more α-ketoglutarate in oxidative decarboxylation, which would result in less α-ketoglutarate participating in toxin biosynthesis. Meanwhile the up-regulation of dihydrolipoamide succinyltransferase might result in less succinate being produced, which would also limit the biosynthesis of PSP toxin. Furthermore, succinyl-CoA synthetase subunit beta was also found to be up-regulated in ACHK-NT. This enzyme catalyzes ATP, succinate and CoA to produce ADP, phosphate and succinyl-CoA [37]. In the last step of the biosynthesis of PSP toxin in cyanobacteria, succinate with compound F' [7] was converted into STX and fumarate under the action of *sxtW* (ferredoxin), *sxtH/T* (phenylpropionate dioxygenase) and *sxtV* (fumarate reductase) individually and simultaneously [8,9]. The up-regulation of succinyl-CoA synthetase might compete with

Table 1 – The differential expression proteins between ACHK-T and ACHK-N.

Spot ID [a]	Protein name [species]	Accession no. [b]	Sequence coverage	Av. ratio [c]	Functional term
Up-regulated protein					
U28	3-Phosphoshikimate 1-carboxyvinyltransferase protein [*Rhizobium etli* Brasil 5]	gi|218507783	17%	2.2	Amino acid metabolism
U33	S-adenosylmethionine synthetase [*Alexandrium minutum*]	gi|112819973	16%	1.55	Amino acid metabolism
U2	Glyceraldehyde-3-phosphate dehydrogenase, type I [*Campylobacter upsaliensis* RM3195]	gi|57505272	13%	1.51	Carbohydrate metabolic process
U18	Hypothetical protein CHLNCDRAFT_56532 [*Chlorella variabilis*]	gi|307111493	4%	1.78	Carbohydrate metabolic process
U45	Phosphoenolpyruvate synthase	gi|218248015	1%	1.86	Carbohydrate metabolic process
U3	Chloroplast transketolase [*Heterocapsa triquetra*]	gi|58613541	8%	1.78	Carbon fixation
U5	Chloroplast transketolase [*Heterocapsa triquetra*]	gi|58613541	9%	1.79	Carbon fixation
U6	Chloroplast transketolase [*Heterocapsa triquetra*]	gi|58613541	8%	1.7	Carbon fixation
U36	Chloroplast phosphoribulokinase [*Pyrocystis lunula*]	gi|60101676	16%	1.92	Carbon fixation
U34	Fructose-bisphosphate aldolase [*Pfiesteria piscicida*]	gi|255965354	71%	2.35	Carbon fixation
U4	Chloroplast transketolase [*Heterocapsa triquetra*]	gi|58613541	75%	1.73	Carbon fixation
U20	Phosphoenolpyruvate carboxykinase [*Naegleria gruberi*]	gi|290993663	8%	1.81	Carbon fixation
U44	Hypothetical protein [*Podospora anserina* S mat+]	gi|171681249	80%	1.75	Carbon utilization
U9	ATP-dependent metalloprotease FtsH [*Rhodothermusmarinus* DSM 4252]	gi|268316402	9%	1.99	Macromolecule catabolic process
U12	ATP-dependent metalloprotease FtsH [*Kosmotogaolearia* TBF 19.5.1]	gi|239617940	6%	1.58	Macromolecule catabolic process
U22	Alkyldihydroxyacetonephosphate synthase, putative [*Treponema denticola* ATCC 35405]	gi|42525657	3%	1.54	Oxidation-reduction process
U17	Glucose–methanol–choline oxidoreductase [*Paracoccus denitrificans* PD1222]	gi|119383846	64%	1.79	Oxidation-reduction process
U48	Ubiquinol-cytochrome C reductase complex 14 kD subunit, putative [*Perkinsus marinus* ATCC 50983]	gi|294872348	83%	1.82	Oxidative phosphorylation
U50	Light-harvesting protein [*Symbiodinium* sp. clade C3]	gi|306430541	9%	2.73	Photophosphorylation
U30	Reconstructed ancestral elongation factor Tu ML-stem [synthetic construct]	gi|32186880	9%	2.08	Protein synthesis
U49	Glutaredoxin-related protein [*Oxyrrhis marina*]	gi|157093557	71%	1.82	Regulation of biological process
U10	Transcriptional regulator protein [*Agrobacterium vitis* S4]	gi|222149504	6%	1.59	Regulation of biological process
U7	Hsp70 [*Crypthecodinium cohnii*]	gi|20143982	37%	1.94	Stress response
U38	Heat shock protein 90 [*Spumella uniguttata*]	gi|38884999	11%	1.58	Stress response
U41	Heat shock protein 90 [*Gymnodinium chlorophorum*]	gi|99643827	8%	2.05	Stress response
U42	Heat shock protein 90 1 [*Alexandrium fundyense*]	gi|134037070	36%	2.24	Stress response
U43	Heat shock protein 90 [*Karlodinium micrum*]	gi|112253669	8%	1.73	Stress response
U26	Ferritin and Dps [*Stappia aggregata* IAM 12614]	gi|118591671	5%	1.55	Stress response
U11	Dihydrolipoamide succinyltransferase, putative [*Perkinsus marinus* ATCC 50983]	gi|294945867	70%	1.57	TCA cycle
U54	Succinyl-CoA synthetase subunit beta [*Thermobifida fusca* YX]	gi|72162976	7%	1.81	TCA cycle
U1	Transitional endoplasmic reticulum ATPase protein [*Cryptosporidium muris* RN66]	gi|209880048	23%	1.65	Transporters
U27	F1-ATP synthase beta chain [alpha proteobacterium BAL199]	gi|163792320	19%	2.18	Transporters
U37	Magnesium chelatase ATPase subunit I [*Synechococcus* sp. WH 5701]	gi|87302130	26%	2.2	Transporters
U56	ATP synthase subunit A [*Ketogulonicigenium vulgar* Y25]	gi|308754148	9%	2.2	Transporters
U32	ABC transporter related protein [*Streptomyces* sp. ACT-1]	gi|282872184	8%	1.73	Transporters

(continued on next page)

Table 1 *(continued)*

Spot ID [a]	Protein name [species]	Accession no. [b]	Sequence coverage	Av. ratio [c]	Functional term
U31	SH3 type 3 domain-containing protein [*Pseudomonas syringae* pv. *syringae* 642]	gi|302185609	41%	2.94	Unclassified
U47	Conserved hypothetical protein [*Noctiluca scintillans*]	gi|157093403	13%	1.66	Unclassified
U21	Conserved hypothetical protein [*Perkinsus marinus* ATCC 50983]	gi|294897078	92%	1.65	Unclassified
U55	Hypothetical protein AURANDRAFT_35132 [*Aureococcus anophagefferens*]	gi|323446392	59%	1.81	Unclassified
U24	Predicted protein [*Micromonas pusilla* CCMP1545]	gi|303286529	8%	1.53	Unclassified
U35	Tetrathionate reductase complex, subunit C [*Providencia rettgeri* DSM 1131]	gi|291326371	2%	1.54	Unclassified
U53	Precursor of synthetase [*Thalassiosira pseudonana* CCMP1335]	gi|223993443	6%	2.36	Unclassified
Down-regulated protein					
D7	Luciferin-binding protein [*Alexandrium catenella*]	gi|166030338	45%	−3.08	Bioluminescence
D8	Luciferin-binding protein [*Alexandrium catenella*]	gi|166030338	56%	−4.61	Bioluminescence
D10	Luciferin-binding protein [*Alexandrium catenella*]	gi|166030338	38%	−5.31	Bioluminescence
D11	Luciferin-binding protein [*Alexandrium catenella*]	gi|166030338	43%	−1.67	Bioluminescence
D12	Luciferin-binding protein [*Alexandrium catenella*]	gi|166030338	37%	−2.76	Bioluminescence
D14	Luciferin-binding protein [*Alexandrium catenella*]	gi|166030338	37%	−3.29	Bioluminescence
D15	Luciferin-binding protein [*Alexandrium catenella*]	gi|166030338	28%	−4.85	Bioluminescence
D16	Luciferin-binding protein [*Alexandrium catenella*]	gi|166030338	26%	−3.33	Bioluminescence
D17	Luciferin-binding protein [*Alexandrium catenella*]	gi|166030338	24%	−11.04	Bioluminescence
D21	Polyketide synthase [*Prorocentrum micans*]	gi|194354512	27%	−1.87	Biosynthesis of secondary metabolites
D2	Molecular chaperone DnaK [*Thermosynechococcus elongatus* BP-1]	gi|22299276	98%	−2.17	Chaperone
D28	Conserved hypothetical protein [*Perkinsus marinus* ATCC 50983]	gi|294941730	85%	−1.6	Cofactor metabolic process
D24	Geranylgeranyl reductase [*Oscillatoria* sp. PCC 6506]	gi|300864352	9%	−1.68	Heterocycle metabolic process
D26	Chloroplast ferredoxin-NADP(+) reductase [*Heterocapsa triquetra*]	gi|58613455	72%	−1.5	Oxidation-reduction process
D29	Hypothetical protein AURANDRAFT_69941 [*Aureococcus anophagefferens*]	gi|323449109	82%	−1.59	Protein modification process
D18	GAF sensor hybrid histidine kinase [*Candidatus Solibacter usitatus Ellin*6076]	gi|116621165	2%	−1.53	Signal transduction
D23	Hybrid signal transduction histidine kinase J [*Stigmatella aurantiaca* DW4/3-1]	gi|310824799	1%	−2.22	Signal transduction
D31	Eukaryotic initiation factor 4E [*Pfiesteria piscicida*]	gi|112253385	10%	−1.51	Translation
D4	Fibronectin type III domain-containing protein [*Campylobacter jejuni* subsp. *doylei* 269.97]	gi|153951256	13%	−2.43	Unclassified
D6	Unnamed protein product [*Sordaria macrospora*]	gi|289616226	14%	−1.51	Unclassified
D9	Hypothetical protein SORBIDRAFT_01g045470 [*Sorghum bicolor*]	gi|242036749	6%	−2.33	Unclassified
D19	Hypothetical protein FsymDgDRAFT_0466 [*Frankia symbiont* of *Datisca glomerata*]	gi|289641039	4%	−1.65	Unclassified
D22	Conserved hypothetical protein [*Neospora caninum* Liverpool]	gi|325119245	5%	−1.61	Unclassified
D32	Viviparous-14 [*Zea mays*]	gi|226533288	2%	−1.63	Unclassified
D33	Enhancer of PolyComb-like family member (epc-1) [*Caenorhabditis elegans*]	gi|71992345	3%	−1.52	Unclassified

[a] Spot ID represents the protein spot number on the 2-D DIGE gels.
[b] Accession numbers according to the NCBI database.
[c] Spot abundance is expressed as the average ratio of intensities of up-regulated (positive values) or down-regulated (negative values) proteins at ACHK-NT.

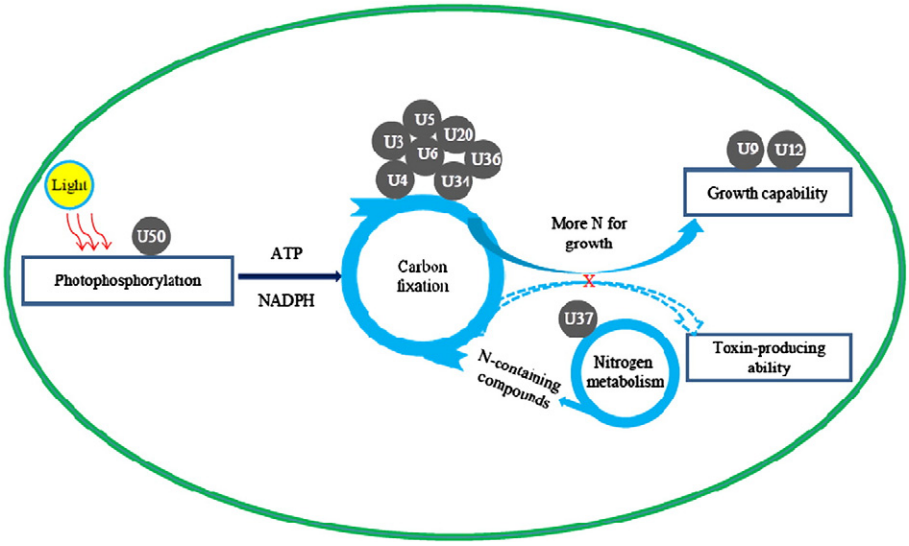

Fig. 7 – Enhancement of certain biological processes related to the growth capability of ACHK-NT. Gray circles are up-regulated proteins in ACHK-NT. More nitrogen compounds and energy were utilized to support cell growth than toxin production in the mutant *A. catenella*.

succinate's role in the biosynthesis of PSP and thus reduce the flow of succinate into the PSP toxin biosynthesis pathway. Together with a low yield of succinate caused by dihydrolipoamide succinyltransferase, the above would contribute to a sharp drop in toxin production. Moreover, chloroplast ferredoxin-NADP(+) reductase was suppressed in ACHK-NT. This enzyme catalyzes reduced ferredoxin and NADP(+) to oxidized ferredoxin, NADPH and H^+, which provides H^+ for toxin synthesis in steps 5 and 8 of the PSP toxin biosynthesis pathway in cyanobacteria. Down-regulation of this enzyme might decrease the production of H^+ and subsequently inhibit PSP toxin biosynthesis in ACHK-NT.

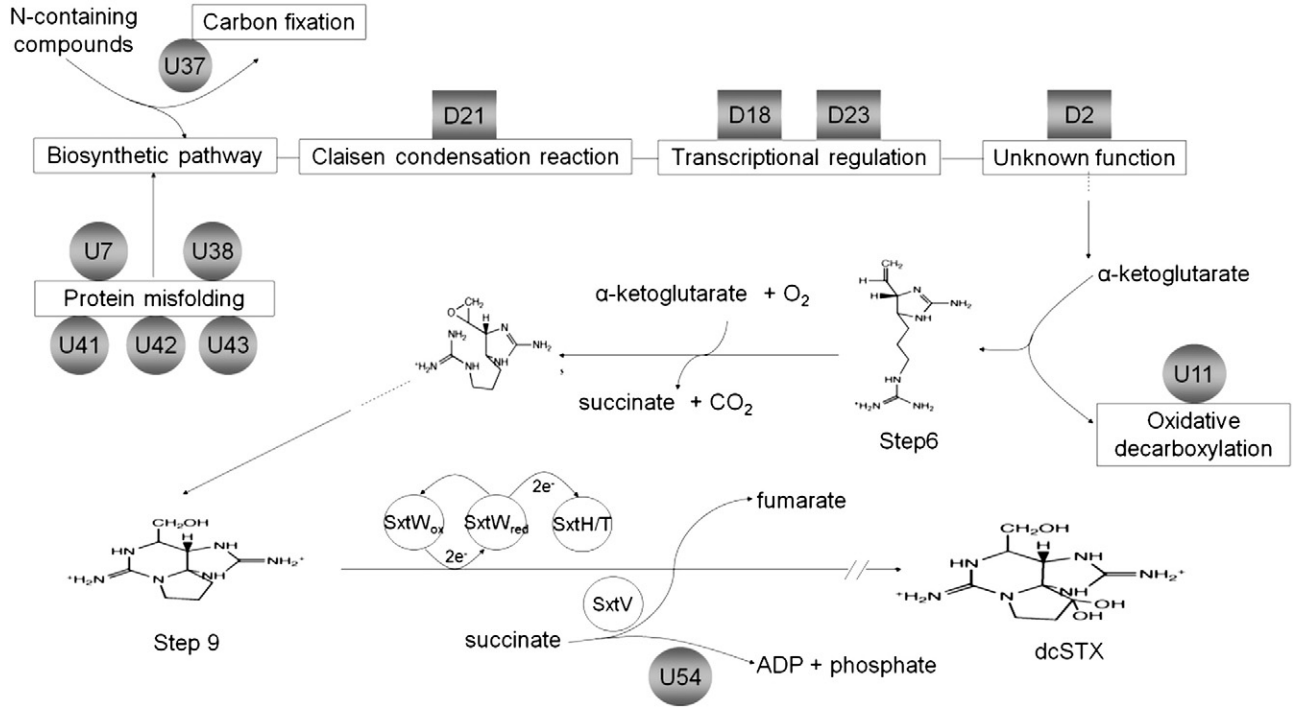

Fig. 8 – Depression of essential reactions upstream or downstream of the biosynthetic pathway of PSP toxins in the mutant ACHK-NT. Chemical structures or reactions in the PST biosynthesis pathway are cited from Mihali et al. [9]: gray rectangles are down-regulated proteins, and gray circles are up-regulated proteins in ACHK-NT.

4.4. *Biological roles of other differentially expressed proteins in the mutant A. catenella*

Five protein spots identified as HSPs were consistently highly expressed in ACHK-NT. HSP90 is a member of the HSP family which is enhanced in response to stress caused by heating, dehydrating or by other factors [38]. The function of Hsp90 includes assisting in protein folding [31], cell signaling, protein degradation [39,40] and interaction with steroid receptors [41–43]. HSP70 is also an important part of the cell's machinery for protein folding, and helps to protect cells from stress. In this study, the high expression of HSPs in ACHK-NT might be in response to the protein misfolding occurring in the cells as a result of the high metabolic activities involved in cell growth in the mutant ACHK-NT. High expression of HSPs has also been linked to stress responses. Therefore, high expression of HSPs was not surprising in ACHK-NT, since the loss of toxicity might break the intracellular balance and induce stress to cells, and so HSPs initiate the protection mechanism to shield cells from damage or to acclimatize to stresses.

Interestingly, nine LBP isoforms were remarkably down-regulated in ACHK-NT. LBP is a key protein regulating luminescence in dinoflagellates, and stabilizes luciferin, a high-energy substrate, from being spontaneously oxidized at a neutral pH. It should be noted that luciferin is a tetrapyrrole containing four five-member rings of one nitrogen and four carbons, and its oxidation, catalyzed by luciferase, produces N-rich intermediate products with a similar structure to PSP toxins, which might provide precursors for toxin biosynthesis, suggesting that a potential relationship might exist between the bioluminescence pathway and the toxin biosynthesis pathway in PSP producing dinoflagellates. The down-regulation of LBP might reduce the production of N-enrichment intermediate products, which would limit toxin biosynthesis. Besides LBP, another protein, ATP-dependent metalloprotease FtsH, was enhanced in ACHK-NT. In *Escherichia coli*, the ftsH gene is involved in the localization processes of some envelope proteins (folding, assembly ortopogenesis for PBP3 and membrane translocation for P-lactamase) and is essential for cell growth [44]. The enhancement of FtsH in ACHK-NT indicated that it might play key roles in regulating cell growth.

It should be pointed out that more than twenty proteins were not identified and their functions are unknown, and yet these proteins might be involved in various biological processes including toxin biosynthesis. In the present study, comparison of the proteomics between mutant and wild subcultures was restricted to the exponential growth phase, whereas broad-ranging sampling times in the cell cycle or growth phase, or in different culture conditions, may provide more important and interesting information on the PSP toxin and dinoflagellate proteomics research. In the future, it is expected that increases in both genetic information and the protein database will help to reveal the functions of these unidentified proteins and their roles in dinoflagellates.

5. Conclusions

The present study for the first time compared the protein profiles of toxicity-lost mutant and wild type *A. catenella* using a quantitative proteomic approach, and identified differentially expressed proteins in the mutant *A. catenella*. Among the altered proteins, those involved in carbon fixation and growth related biological processes were up-regulated in the mutant *A. catenella*, while proteins participating in toxin biosynthesis and related biological processes were down regulated. The differences in these biological processes between the toxicity-lost mutant and the wild type *A. catenella* might explain the loss of toxicity in the former. The depression of essential reactions upstream or downstream of the toxin biosynthetic pathway might block toxin production and result in the loss of toxin-producing ability in the mutant *A. catenella*. This study suggested that toxin biosynthesis is a complex and comprehensive process which involves various biological processes, such as photosynthesis, carbon fixation, and nitrogen assimilation. In the future, we will compare transcriptomic profiles between mutant and wild *A. catenella* to identify unique genes as well as highly abundant genes in wild *A. catenella* which, when combined with the proteomic data, might help to reveal more concerning the toxin biosynthesis mechanism and pathway.

Supplementary data to this article can be found online at http://dx.doi.org/10.1016/j.jprot.2012.08.001.

Acknowledgments

This work was partially supported by research grants from the National Natural Science Foundation of China (41176094 and 40776068), the Ministry of Science and Technology of the People's Republic of China (project no. 2010CB428703), the Excellent Group and the Program for New Century Excellent Talents in University to D.-Z. Wang. We thank HF Gu and ZH Luo for their assistance during DNA sequence analysis, and Professor John Hodgkiss from The University of Hong Kong for his help with the English used in this paper.

REFERENCES

[1] Taylor F, Fukuyo Y. The neurotoxigenic dinoflagellate genus *Alexandrium halim*: general introduction. Physiological Ecology of Harmful Algal Blooms, 41; 1998. p. 3–12.
[2] Hallegraeff GM. A review of harmful algal blooms and their apparent global increase. Phycologia 1993;32:79-99.
[3] Cho Y, Hiramatsu K, Ogawa M, Omura T, Ishimaru T, Oshima Y. Non-toxic and toxic subclones obtained from a toxic clonal culture of *Alexandrium tamarense* (Dinophyceae): toxicity and molecular biological feature. Harmful Algae 2008;7:740-51.
[4] Moustafa A, Loram J, Hackett J, Anderson D, Plumley F, Bhattachary D. Origin of saxitoxin biosynthetic genes in cyanobacteria. PLoS One 2009;4:e5758.
[5] Yang I, John U, Beszteri S, Glöckner G, Krock B, Goesman A, et al. Comparative gene expression in toxic versus non-toxic strains of the marine dinoflagellate *Alexandrium minutum*. BMC Genomics 2010;11:1–18.
[6] Taroncher-Oldenburg G, Kulis D, Anderson D. Toxin variability during the cell cycle of the dinoflagellate *Alexandrium fundyense*. Limnol Oceanogr 1997;42:1178-88.
[7] Taroncher-Oldenburg G, Anderson D. Identification and characterization of three differentially expressed genes, encoding S-adenosylhomocysteine hydrolase, methionine

aminopeptidase, and a histone-like protein, in the toxic dinoflagellate *Alexandrium fundyense*. Appl Environ Microbiol 2000;66:2105-12.
[8] Kellmann R, Mihali TK, Jeon YJ, Pickford R, Pomati F, Neilan BAF. Biosynthetic intermediate analysis and functional homology reveal a saxitoxin gene cluster in cyanobacteria. Appl Environ Microbiol 2008;74:4044-53.
[9] Mihali TK, Kellmann R, Neilan BA. Characterisation of the paralytic shellfish toxin biosynthesis gene clusters in *Anabaena circinalis* AWQC 131 C and *Aphanizomenon* sp. NH-5. BMC Biochem 2009;10:8.
[10] Stucken K, John U, Cembella AD, Murillo A, Soto-Liebe K, Friedel M, et al. The smallest known genomes of multicellular and toxic cyanobacteria: comparison, minimal gene sets for linked traits and the evolutionary implications. PLoS One 2010;5:e9235.
[11] Harlow L, Koutoulis A, Hallegraeff G. S-adenosylmethionine synthetase genes from eleven marine dinoflagellates. Phycologia 2007;46:46-53.
[12] Stüken A, Orr RJS, Kellmann R, Murray SA, Neilan BA, Jakobson KS. Discovery of nuclear-encoded genes for the neurotoxin saxitoxin in dinoflagellates. PLoS One 2011;6:e20096.
[13] Lee FWF, Lo SCL. Proteomic study of micro-algae: sample preparation for two-dimensional gel electrophoresis and de novo peptide sequencing using MALDI-TOF MS. Curr Proteomics 2007;4:67-78.
[14] Wang DZ, Li C, Dong HP, Xie ZX, Lin L, Hong HS. Homology-driven proteomics of dinoflagellates with unsequenced genome by MALDI-TOF /TOF and automated de novo sequencing. Evid-Based Complement Altern Med 2011, doi:10.1155/2011/ 471020.
[15] Tannu NS, Hemby SE. Two-dimensional fluorescence difference gel electrophoresis for comparative proteomics profiling. Nat Protoc 2006;1(4):1732-42.
[16] Li C, Wang DZ, Dong HP, Xie ZX, Hong HS. Proteomics of a toxic dinoflagellate *Alexandrium catenella* DH01: detection and identification of cell surface proteins using fluorescent labeling. Chin Sci Bull 2012;57(1):1-8, doi:10.1007/s11434-012-5156-5.
[17] Wang DZ, Dong HP, Li C, Xie ZX, Lin L, Hong HS. Identification and characterization of cell wall proteins of a toxic dinoflagellate *Alexandrium catenella* using 2-D DIGE and MALDI TOF–TOF mass spectrometry. Evid-Based Complement Altern Med 2011, doi:10.1155/2011/984080.
[18] Keller M, Selvin R, Claus W, Guillard R. Media for the culture of oceanic ultraphytoplankton. J Phycol 1987;23:633-8.
[19] Fritz L, Triemer RE. A rapid simple technique utilizing Calcofluor white M2R for the visualization of dinoflagellate thecal plates. J Phycol 1985;21:662-4.
[20] Adachi M, Sake Y, Ishida Y. Analysis of *Alexandrium* (Dinophyceae) species using sequences of the 5.8S ribosomal DNA and internal transcribed spacer regions. J Phycol 1996;32(3):424-32.
[21] Altschul S, Madden T, Schaffer A, Zhang J, Zhang Z, Miller W, et al. Gapped BLAST and PSI-BLAST: a new generation of protein database search programs. Nucleic Acids Res 1997;25:3389-402.
[22] Wang DZ, Zhang SG, Gu HF, Chan LL, Hong HS. Paralytic shellfish toxin profiles and toxin variability of the genus *Alexandrium* (Dinophyceae) isolated from the Southeast China Sea. Toxicon 2006;48:138-51.
[23] Wang DZ, Lin L, Chan LL, Hong HS. Comparative studies of four protein preparation methods for proteomic study of the dinoflagellate *Alexandrium* sp. using two-dimensional electrophoresis. Harmful Algae 2009;8:685-91.
[24] Shevchenko AH. In-gel digestion for mass spectrometric characterization of proteins and proteomes. Nat Protoc 2007;1:2856-60.
[25] Toulza E, Shin MS, Blanc G, Audic S, Laabir M, Collos Y, et al. Gene expression in proliferating cells of the dinoflagellate *Alexandrium catenella* (Dinophyceae). Appl Environ Microbiol 2010;76:4521–4529.25.
[26] Martins CA, Kulis D, Franca S, Anderson DM. The loss of PSP toxin production in a formerly toxic *Alexandrium lusitanicum* clone. Toxicon 2004;43:195-205.
[27] Wang DZ, Jiang TJ, Hsieh DPH. Toxin composition variations in cultures of *Alexandrium* species isolated from the coastal waters of Southern China. Harmful Algae 2005;4(1):109-21.
[28] Omura T, Onodera H, Ishimaru T, Oshima Y. Non-toxic mutational strains in the paralytic shellfish poisoning causative dinoflagellates, *Alexandrium* spp. La Mer 2003;41:86-93.
[29] Ogata T, Kodama M, Ishimaru T. Toxin production in the dinoflagellate *Protogonyaulax tamarensis*. Toxicon 1987;25:923-8.
[30] Stauber EI, Fink A, Markert C, Kruse O, Johanningmeier U, Hippler M. Proteomics of *Chlamydomonas reinhardtii* light-harvesting proteins. Eukaryot Cell 2003;2:978-94.
[31] Flynn K, Franco JM, Fernandez P, Reguera B, Zapata M, Wood G, et al. Changes in toxin content, biomass and pigments of the dinoflagellate *Alexandrium minutum* during nitrogen refeeding and growth into nitrogen or phosphorus stress. Mar Ecol Prog Ser 1994;111:99–109.
[32] Granéli E, Johansson N, Panosso R. Cellular toxin contents in relation to nutrient conditions for different groups of phycotoxins. In: Reguera B, Blanco J, Fernández ML, Wyatt T, editors. Harmful Algae. Xunta de Galicia and Intergovern. Oceanographic Comm. of UNESCO; 1998. p. 321-4.
[33] Cembella AD. Ecophysiology and metabolism of paralytic shellfish toxins in marine microalgae. In: Anderson DM, Cembella AD, Hallegraeff GM, editors. Physiological ecology of harmful algal blooms. Heidelberg: Springer Verlag; 1998. p. 381-404.
[34] Uribe P, Espejo RT. Effect of associated bacteria on the growth and toxicity of *Alexandrium catenella*. Appl Environ Microbiol 2003;69:659-62.
[35] Lu YH, Chai TJ, Hwang DF. Isolation of bacteria from toxic dinoflagellate *Alexandrium minutum* and their effects on algae toxicity. J Nat Toxins 2000;9:409-17.
[36] Hold GL, Smith EA, Birkbeck TH, Gallacher S. Comparison of paralytic shellfish toxin (PST) production by the dinoflagellates *Alexandrium lusitanicum* NEPCC 253 and *Alexandrium tamarense* NEPCC 407 in the presence and absence of bacteria. FEMS Microbiol Ecol 2001;36:223-34.
[37] Lykidis A, Mavromatis K, Ivanova N, Anderson I, Land M, DiBartolo G, et al. Genome sequence and analysis of the soil cellulolytic actinomycete *Thermobifida fusca* YX. J Bacteriol 2007;189:2477-86.
[38] Prodromou C, Panaretou B, Chohan S, Siligardi G, O'Brien R, Ladbury JE, et al. The ATPase cycle of Hsp90 drives a molecular 'clamp' via transient dimerization of the N-terminal domains. EMBO J 2000;19:4383-92.
[39] Buchner J. Hsp90 & Co.—a holding for folding. Trends Biochem Sci 1999;24:136-41.
[40] Imai J, Maruya M, Yashiroda H, Yahara I, Tanaka K. The molecular chaperone Hsp90 plays a role in the assembly and maintenance of the 26S proteasome. EMBO J 2003;22:3557-67.
[41] Kimura Y, Matsumoto S, Yahara I. Temperature-sensitive mutants of Hsp82 of the budding yeast *Saccharomyces cerevisiae*. Mol Gen Genet 1994;242:517-27.
[42] Pratt W, Morishima Y, Murphy M, Harrell M. Chaperoning of glucocorticoid receptors. Mol Chaperones Health Dis 2006;172:111-38.
[43] Grad I, Picard D. The glucocorticoid responses are shaped by molecular chaperones. Mol Cell Endocrinol 2007;275:2–12.
[44] Tomoyasu T, Yuki T, Morimura S, Mori H, Yamanaka K, Niki H, et al. The *Escherichia coli* FtsH protein is a prokaryotic member of a protein family of putative ATPases involved in membrane functions, cell cycle control, and gene expression. J Bacteriol 1993;175:1344-51.